In: Advances in Semiconductor Research
Editors: D. Persano Adorno and S. Pokutnyi
ISBN: 978-1-63321-755-3

Chapter 1

QUANTUM SIZE EFFECTS IN SEMICONDUCTOR NANOCRYSTALS

Faming Gao [*] ***and Lihua Gao***
Key Laboratory of Applied Chemistry,
Yanshan University, Qinhuangdao, China

Abstract

Most semiconducting clusters show size-dependence effects in the nanometer region. Along with the energy gap of the cluster, the photoluminescence can even be varied through the red to blue region of the visible spectrum. Quantum size effects in semiconductor clusters have been a subject of extensive studies for the last two decades. We review recent developments of theoretical studies on the quantum size effects. The useful theoretical models based on the exciton confinement such as Effective-mass approximation (EMA), Empirical tight-binding method (ETBM) and Empirical pseudopotential method (EPM) have been established. In particular, a chemical bond method of quantum confinement is introduced in detail. In order to calculate readily the energy-gap shifts for clusters of all size, this method express the effects through algebraic relations rather than through variational solutions of the wave equation. It shows that a competition between the positive Kubo energy-gap shift and the negative surface energy shift plays the crucial role in the optical gaps of the nanosystems.

Keywords: quantum size effects, nanocrystals, semiconductor, chemical bond

Introduction

For the last two decades, semiconductor nanocrystals have attracted considerable interest due to their unique properties and potential use in the fields of nonlinear optics, luminescence, electronics, catalysis, solar energy conversion, and optoelectronics[1-3]. Current researches in semiconductor nanocrystals are mainly focused on the improved and controlled clusters growth, suitable process technologies, unique materials characterization, and better

[*] E-mail address: fmgao@ysu.edu.cn. Corresponding Author Address: No. 438 Hebei Street, Qinhuangdao, 066004, Hebei Province, China.

understanding of the structure-property relationships. Further research of nanotechnology will certainly lead to significant breakthrough in semiconductor industry. The development of new semiconductor clusters depends not only on materials engineering at a practical level, but also on a comprehensive understanding of the properties of materials, as well as the fundamental science behind these properties. Structure-property relationships have always been the intrinsically and most important aspect to materials science and engineering.

Reducing the size of semiconductor to nanometer range leads to the appearance of quantum size effect, surface effect, small-size effect, macroscopic quantum tunneling effect, dielectric confinement effect, etc., in which quantum size effect has been one of the most studied subjects, both in practice and theory. Quantum size effect gives rise to the discrete energy levels depending on the size of the structure as it is known from the simple potential well treated in introductory quantum mechanics. Among many properties that exhibit a dependence upon size in semiconductor cluster, blue shift (increase) of band gap energy is of particular importance. Along with the energy-gap of the cluster, the photoluminescence can even be varied through the red to the blue region of the visible spectrum. Thus, this allows scientists the unique opportunity to tune the electronic and chemical properties of a material simply by controlling its particle size. Theoretically, predicting accurately the spectra of clusters as a function of their size is one of the fundamental nanoscientific issues, and of utmost importance.

The pioneering work to allow for the influence of size quantization on interband absorption in a semiconductor sphereis the Effective Mass Approximation (EMA) proposed by Al. L. Efros and A. L. Efros [1]. It assumes a particle in a potential well with an infinite potential barrier at the particle boundary. Three size regimes on the basis of quantum scales are identified:

Firstly, when the radius R of a semiconductor is less than the Bohr radii of electrons a_e, and holes a_h, the blue shift can be expressed as [1]:

$$\Delta E = \frac{\hbar^2 \pi^2}{2\mu R^2} \tag{1}$$

where μ is the reduced mass of an electron-hole pair. The magnitude of Coulomb attraction can be neglected due to that the kinetic energy of localization is much larger, and this case is termed Strong Confinement.

Secondly,when a_h<R<a_e,the shift is expressed as:

$$\Delta E = \frac{\hbar^2 \pi^2}{2m_e R^2} \tag{2}$$

here m_e is the effective electron mass, and this is the heavy hole case.

Thirdly, when R >{ a_e, a_h },

$$\Delta E = \frac{\hbar^2 \pi^2}{2MR^2} - E_{Rg}^{*} \tag{3}$$

M is the total mass of electron m_e and hole m_h, and E_{Rg}^* is the effectiveRydberg energy:

$$E_{Rg}^* = \frac{e^4}{2\varepsilon^2\hbar^2(m_e^{-1} + m_h^{-1})} \tag{4}$$

This case is termed Weak Confinement. In the EMA model, the energy band is parabolic near the band-edge.

Later Brus[5-7] modified the EMA model and proposed the following expression for the band gap shift of the finite sized system:

$$\Delta E_g = \frac{\hbar^2\pi^2}{2R^2}\left(\frac{1}{m_e} + \frac{1}{m_h}\right) - 1.786\frac{e^2}{\varepsilon R} - 0.248E_{Rg}^* \tag{5}$$

The first term is the kinetic energy of both the electron and the hole, representing a relationship between quantum localization energy or confinement energy and the radius *R*. The second term shows the Columbic interaction energy between the electron and hole. ε is the dielectric constant. The third term is size independent and is generally small compared to the other two terms, which can be negligible, except for the semiconductors with small dielectric constant [2]. According to Eq. (5), the band gap increases as the quantum dot radius decreases, since that the quantum localization term shifts to higher energy with decreased *R*, meanwhile the Columbic term shifts excited electronic state to lower value. The EMA model apparently provides a good understanding for the blue shift of the optical absorption threshold. However, this model is suitable only for very large nanocrystals. When *R* decreases to a small regime, the eigenvalues of the lowest excited states are located in a region of the energy band that is no longer be approximated as parabolic, and the EMA model breaks down. This model gives quantitatively accurate results only for very large clusters [1]. Hence, there is a need for microscopic calculations geared towards mapping out the energy-level structure of these clusters and explain the salient features of their absorption spectra. Krishna et al., [3, 4] carried out a systematic investigation of quantum confinement effects in clusters using pseudopotentials. Their study provides a global understanding of the changes taking place in the electronic structure of clusters as the cluster dimensions, crystal structure, physical shape, and the lattice constant are varied. Pokutnyi[5-7] proposed a modified effective mass approximation to describe the exciton energy spectrum in semiconductor quantum dots with the radii *a* comparable to the exciton Bohr radius a_{ex}^0 .It is shown that, when the reduced effective mass of the excitons is assumed as a function of the radius of the quantum dot, the modified EMA method could be used to describe the exciton for quantum dots with radii $a \approx a_{ex}^0$.

Öğüt et al. [8] have implemented *ab* initio realspace calculations of quasiparticle and local density approximation (LDA) band gaps, self-energy corrections, exciton Coulomb energies, and optical gaps for Si quantum dots with diameters up to 2.72 nm using the higher-order finite pseudopotential method. Their calculated optical gaps are in very good agreement with the optical absorption data from Si nanocrystallites. Although *ab* initio calculations appear to be a more desirable way to investigate the optical gaps of clusters [8],for most nanosystems containing from a few thousands to 10^6 atoms, *ab* initio calculations are still too

laborious to be practical.Wang [9] proposed an empirical tight-binding model (ETBM) to calculate the band gap of PbS with a sp^3pseudofuctions centered on Pb and S atoms, which can give a better description of the band structure and is more adequate for small crystallites. Then Lippens and Lannoo[10] developed the ETBM model to study the size dependence of the band gap for CdS, ZnS and CdSe, using a 13 parameters sp^3s^* model without the spin-orbit interaction. The crystallites observed had a symmetric shape and dangling orbitals were neglected. The recursion method was adopted for the reason that it is an iterative algorithm and does not require the storage of all the elements of Hamiltonian matrix. Ren et al. [11] used the ETBM model to study the electronic structures of surface-hydrogenated Si cluster, by using the group theory to simplify the diagonalization of their matrices. Similar researches demonstrated that the ETBM can give useful information about semiconductor nanocrystals.

There are also other approaches to investigate the size-dependent band gaps of semiconductor clusters, such as the effective bond order method (EBOM)[15, 16], the empirical pseudopotential method (EPM) [12], perturbation theory [13], etc. However, major computational efforts and difficulties do not allow one to calculate the properties of large sized nanocrystals, hence they can only treat thousand-atom electronic structure calculations. Furthermore, almost all existing theoretical calculations for band gap on semiconductor clusters to date assume that interior-to-interior optical transitions dominate the optical properties, neglect the surface effects, and effectively treat the crystal surface as a perfectly reflecting wall [19].Nevertheless, the optical properties of clusters can be significantly affected by the surface states due to the high surface-to-volume ration. A 5nm CdS semiconductor dot has roughly 15% atoms at the surface. Such a high surface-to-volume ratio may induce an enhanced or reduced transfer rate of photogenerated charge carries because of the high density of surface sites which arise from unsatisfied bonds at the reconstructed surface. The energies of these surface states generally lie in the bandgap of the semiconductor dots[20]. Hence, theycan trap charge carriers (electron or hole) and behave as reducing (electron) or oxidizing (hole) agents [14].This behavior at the surface can affect the overall conductivityand optical properties. As a result, surface states have significant effects on the optical andoptoelectronic properties of the semiconductor dots. It would lead to insufficient prediction for the spectra of clusters, and hinder the understanding of novel properties if we neglect the surface effect of semiconductor clusters, especially for those with the dimensions of only a few nanometers.

Methods

Chemical Bond Theory for Quantum Size Effects

Recently, a chemical bond method of quantum confinement effects is proposed to study the band gap of quantum clusters with different sizes and configurations [22, 23].In their opinions, the optical gap shift may be basically decomposed into contributions due to the surface effects and quantum effects, both of which are size dependent. The surface effects have a high correlation with the bonding and fraction of atoms at the surface, and cannot be neglected when the size of semiconductors decreases to nanoscale. The quantum effects are related to the reduction of the band structure into discrete quantum levels because of the limited atoms of the nanocrystals. Consequently, the energy gap shift ΔE, which may be

measured by the shift of absorption threshold of the nanocrystal relative to that of the bulk, can be written as the sum of the quantum effect shift part ΔE^{kubo} and the surface effect shift part $\Delta E^{\text{surface}}$[15]:

$$\Delta E_{\text{g}}(D) = \Delta E^{\text{kubo}} + \Delta E^{\text{surface}} \tag{6}$$

For a bulk crystal, the interaction of an infinite number of atomic orbitals results in a continuum of levels, i.e. band. The numbers of atomic orbitals which take part in combination will become less along with the decrease of crystal size, causing that the band continuum becomes broken down to quantized energy levels. The gap between the highest occupied molecular (HOMO) and the lowest unoccupied molecular orbital (LUMO) energy level may be called the Kubo gap [24]. Accordingly, Kubo energy shiftΔE^{kubo}stems from that the electrons are confined inside a finite volume *V*. An empirical expression for the Kubo energy shift was proposed as follow [15]:

$$\Delta E^{\text{kubo}}=(m_{\text{e}}e^4/2\hbar^2)(VN_{\text{e}})^{-1/3} \tag{7}$$

where N_{e} is the valence electron density of the bonds:

$$N_{\text{e}} = (n_{\text{e}})^* N_{\text{b}} \tag{8}$$

$$n_{\text{e}} = (Z^*_{\text{cation}} / N_{\text{C cation}} + Z^*_{\text{anion}} / N_{\text{C anion}}) \tag{9}$$

N_b is the density of chemical bond (*i.e.*the number of chemical bonds per cubic centimeter) which can be obtained from the crystal structure parameters. $n_{\text{e}}$is the number of effective valence electrons per chemical bond. Z^*_{cation} and Z^*_{anion} are the numbers of effective valence of cation and anion, respectively. $N_{\text{C cation}}$ and $N_{\text{C anion}}$ represents the nearest coordination number of cation and anion, respectively. In nanoscale systems, the average surface atom coordination number equals to the total bond number at the surface divided by the number of the surface atoms in the nanocrystal, which were employed to study the electronic structure of nanocrystal by Mason [16].

On the other hand, the termination of the lattice periodicity in the surface of nanoclusters not only creates a potential boundary but also reduces the coordination number of the surface atoms [17] and increases the ratio of surface-to-volume. For the surface region of semiconductor clusters, the bond length contracts due to the surface coordination number imperfection. It is believed that the bond contraction at the surface and the rise in the surface-to-volume ratio of nanoscaled materials are responsible for some derivatives of properties from the bulk crystals. Here, the structure of a nanoparticle may be classified into two regions: the surface and the inside. The former has large dangling bonds and atoms with imperfect coordination number, while the latter is assumed the same as the bulk. The difference between the surface and the inside of nanoparticles is mainly the coordination number loss in surface, which is just the origin of surface effect. Therefore, from the chemical bond point of view, a nanocluster contains two different kinds of bonds: surface bonds and inside bonds. Since the electron feels the effects of the nanocrystal boundaries in addition to

the periodic potential, the surface energy shift part should be resolved into contributions from the two types of bonds, which may be expressed as [15]:

$$\Delta E^{\text{surface}} = F^{\text{surface}}(E_{\text{g}}^{\text{surface}} - E_{\text{g}}^{\text{bulk}}) \tag{10}$$

where F^{surface} is the fraction of surface bonds composing the nanocluster. $E_{\text{g}}^{\text{surface}}$ and $E_{\text{g}}^{\text{bulk}}$ represent the average gap of the surface bond of the nanocluster and the bulk phase, respectively. These average gaps may be obtained using Phillips' chemical bond theory [18, 19].

Phillips' chemical bond theory is an simple means of obtaining the energy-gaps of semiconductor crystals with reasonable accuracy[27, 28],and hasbeen successfully applied to many aspects, especially those that are difficult to address by first principles technique[20]. For a binary compound, the Hamiltonian and potential may be expressed as [21]:

$$\hat{H} = -\frac{\hbar^2}{2m_e}\nabla^2 + V(\mathbf{r}) \tag{11}$$

$$V(\mathbf{r}) = \sum_G [V_s(G)S_s(\mathbf{G}) + iV_A(G)S_A(\mathbf{G})]\exp(i\mathbf{G}\cdot\mathbf{r}) \tag{12}$$

Here **G** is a reciprocal lattice vector, $S_s(\mathbf{G})$ and $S_A(\mathbf{G})$ are the symmetric and antisymmetric structure factors, and $V_s(G)$ and $V_A(G)$ are the symmetric and antisymmetric form factors. The matrix elements of the Hamiltonian are expressed as [18]:

$$H_{11}=H_{22}=0 \tag{13}$$

$$H_{12}=H_{21}^*=E_{\text{h}}+iC, \tag{14}$$

To first order in $V(\mathbf{r})$, the symmetric, homopolar part $E_{\text{h}}$and the antisymmetric, heteropolar part C arise from the real partand the imaginary partof Eq. (12), respectively. The decomposition of average energy gap E_{g} between the highest occupied and the lowest unoccupied energy level may be:

$$E_{\mathbf{g}}^2 = E_{\mathbf{h}}^2 + C^2 \tag{15}$$

In the case of a pure covalent Group IV clusters, E_{g} just equal to E_{h} due to C=0 by symmetry, and E_{h} is a function of nearest-neighbor distance. Thus E_{g}can be expressed as a function of the bond length d:

$$E_{\mathbf{h}} = 39.74/d^{2.48} \tag{16}$$

where d and E_{h} are in Åand eV, respectively.

$$C = 14.4(\beta \cdot N_C^2) \cdot (Z_{cation}^* - Z_{anion}^*) \exp(-k_s \cdot d/2)/(d/2) \quad (17)$$

$$k_s = 2(3\pi^2 N_e)^{1/6}/(\pi a_B)^{1/2} \quad (18)$$

here βdepends on the crystal structure and can be determined via the long-wave dielectricconstant $\varepsilon(\infty)$ of the crystal. a_B is Bohr radius.N_C is the averagecoordination number.

It is shown from the formulae above that bond length plays an important role in calculating the energygaps and the bond length is different for the surface and inside ones.Here, the bond length data of bulk crystal is taken as the inside bond length, while the bond length data of the crystal-cage with only surface atoms is taken as the outside bond length. Figure 1 is the schematic of a nanocrystal sphere and a crystal-cage with only surface atoms.The geometry optimization by first principles for bulk crystal and the crystal-cage was carried out to determine the bond length for surface and inside of semiconductor clusters.

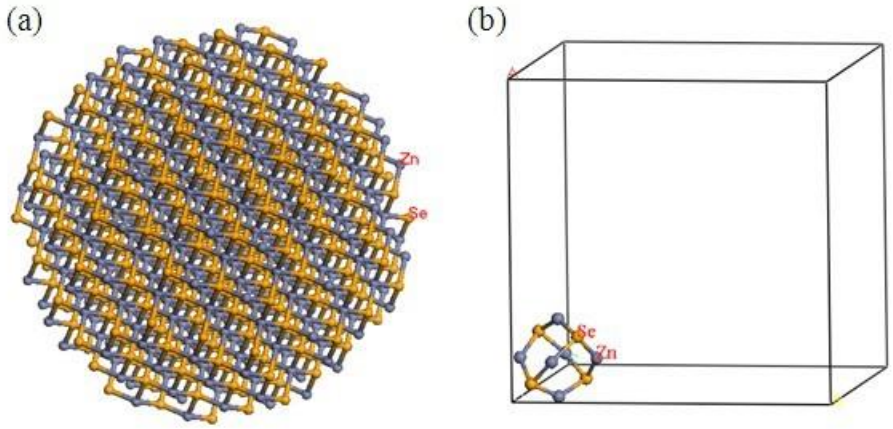

Figure 1. Nanocrystal structure of semiconductor: (a) schematic of a nanocrystal sphere of ZnSe; (b) the crystal-cage of ZnSe with only surface atoms.

The Band Gap Shifts of II-VI, III-V Compound Nanocrystals

CdS, CdSe, ZnS,InP, InAs and GaAs crystals are typical binary semiconductors, whose clusters have been studied using above theory. Figure 2a-f gives the energy gap shifts calculated for CdS, ZnS, InP, InAs, GaAs clusters with zinc blende structure and CdSe clusters with wurtzite sturcute, respectively, as well as the experimental data from other models [15].

Since the change in energy gaps is expressed as a function of the size with respect to that of the bulk, the zero of the energy axis corresponds to the bulk values. The EMA results are shown by the dashed line, which is found to indeed overestimate the bandgaps for InP clusters. While the values calculated from the ETBM model underestimate the experimental energy shifts for the ZnS clusters. What's more, the curve of energy shifts with decreasing cluster size shows a zigzag shape, which is different from traditional results of smooth curves, indicating that the energies do not always shift to blue with decreasing cluster size.

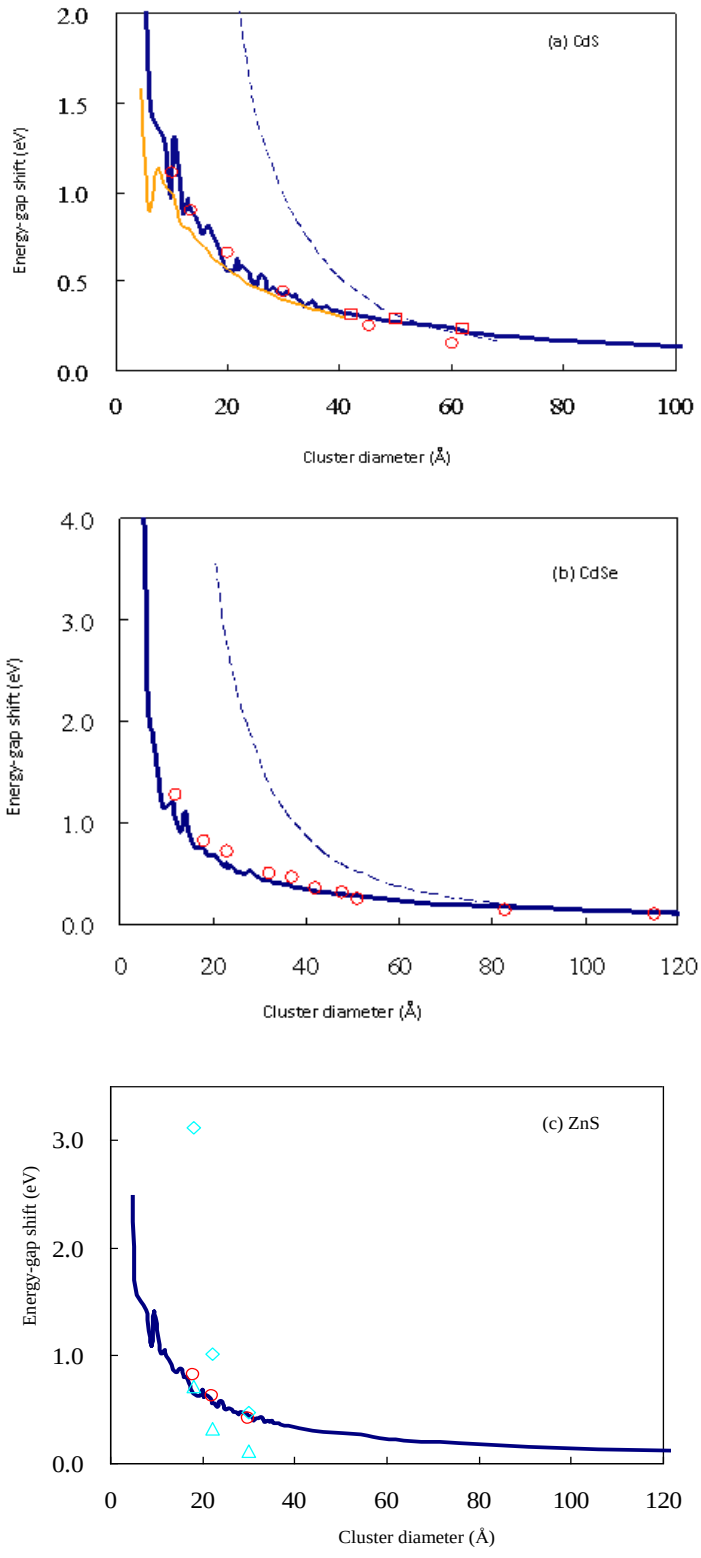

Figure 2. Continued on next page.

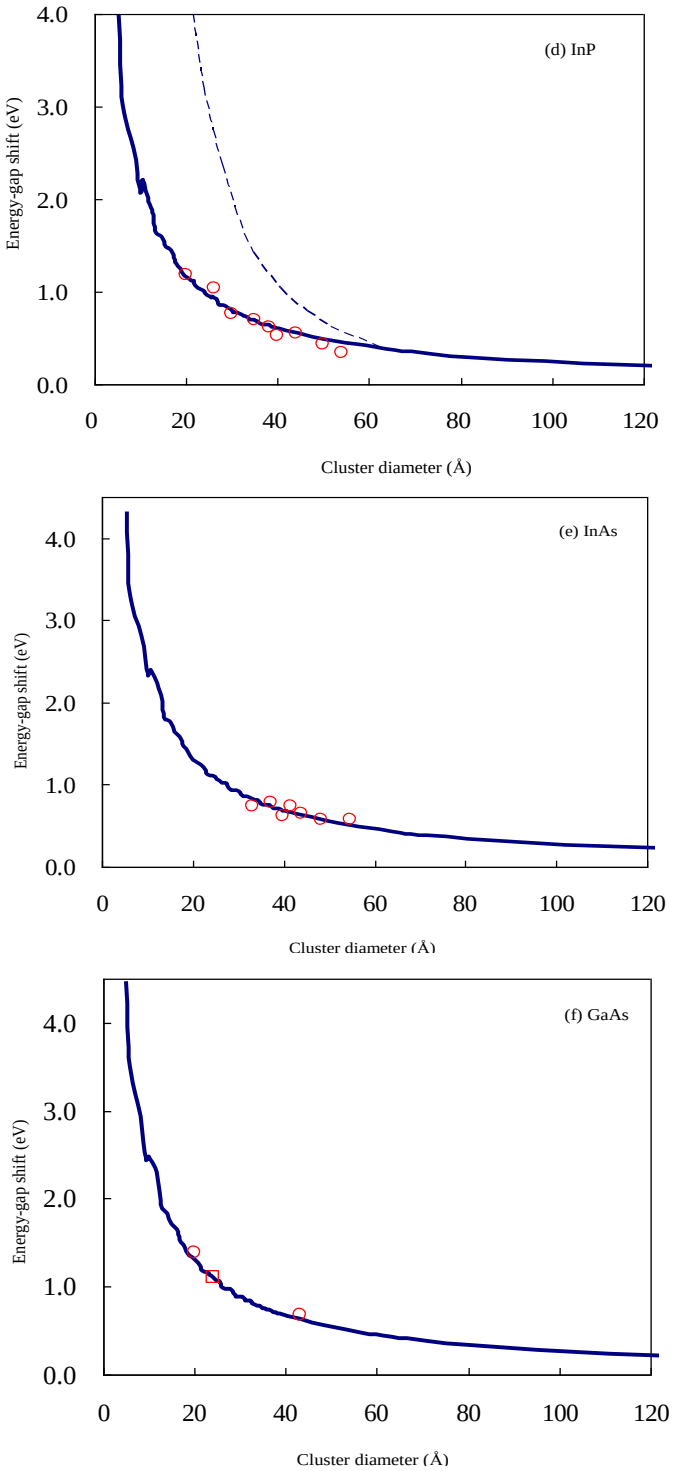

Figure2. Experimental and calculated energy-gap shifts of zinc-blende (a) CdS, (c) ZnS, (d) InP, (e) InAs, (f) GaAs and (b) wurtzite CdSe. The blue solid lines are from the calculations of the spherical clusters using the chemical bond theory. The curves obtained fromEMA are shown by the dashed line. The experimental data are denoted by: (a) ○[2] and □[22]; (b) ○[23]; (c) ○, ◊ from EMA results and △ from ETBM results [24]; (d) ○[25]; (e) ○[26]; (f) ○[27] and □[28].

The Band Gap Shifts of Diamond and Si Nanocrystals

The diamond-cages with the structure of diamondoidsare a unique form of diamond clusters, which attractive unprecedented investigations about the solid state properties as a function of size and shape. The smallest diamondoid is adamantane, and other further members, such as diamantane, triamantane, tetramantane, tetramantane and pentamantane, are derived by adding one face fused cage at a time to the preceding diamondoid structure[38, 39]. The calculated band gap shift ΔE for dimond cages are shown in Table 1. It can be seen that the surface energy shifts for the diamond-cage with the structure of diamondoids are negative values, which slightly reduce the Kubo energy shift. And there is a bit difference in surface energy shifts between two isomers of tetramantane because of different atomic number at the surface [15].

Table 1. Theoretical and experimental energy gap shifts for the carbon cages with the diamondoid structure and the spherical sillicon clusters of different sizes. Energy-gap shift ΔE, kubo energy shift ΔE^{kubo} and surface energy shift $\Delta E^{surface}$ are in eV. The diameter of silicon clusters is D in Å. $\Delta E_{cal}$and ΔE_{exp} are the calculated and experimental results, respectively [15]

diamond cage	ΔE^{kubo}	$\Delta E^{surface}$	ΔE_{cal}	ΔE_{exp}
C_{10}(adamantine)	3.98	-0.31	3.67	3.71
C_{14}(diamantane)	3.55	-0.31	3.25	3.28
C_{16}(triamantane)	3.27	-0.28	2.99	3.01
C_{22}(1(2)3-tetramantane)	3.06	0.25	2.81	2.87
C_{22}(123-tetramantane)	3.06	-0.27	2.79	—
C_{26}(1(2, 3)4-pentamantane)	2.89	-0.21	2.69	2.66
Si (D = 23.1 Å)	1.24	0.02	1.26	1.30
Si (D = 23.9 Å)	1.20	0.01	1.21	1.25
Si (D = 24.3 Å)	1.18	0.02	1.20	1.15
Si (D = 25.0 Å)	1.12	0.01	1.13	1.12
Si (D = 26.8 Å)	1.09	0.01	1.10	1.00
Si (D = 30.4 Å)	0.95	0.01	0.96	0.94

The results of the nano Si with spherical shapes are also shown in Table 1. The surface energy shifts of the nano Si can be neglected as they are very small. Thus, their energy-gap shifts rest with kubo energy shifts. There is a good agreement between the calculated and the experimental results, demonstrating the predictive power of chemical bond method.

The Band Gap Shifts of Oxides Nanocrystals

Titanium oxide (TiO_2) is a well-known photocatalysis materialwhich has been extensively studied with regard to synthesis, properties and applications. Since the catalytic properties may be affected by energy gap shift, the investigation of quantum size effect on band gap is of intense interest. Serpone [29] synthesized anatase TiO_2 nano clusters with

average sizes 2.1, 13.3 and 26.7nm, and characterized the clusters by absorption and photoluminescence spectroscopies. Under their conditions, no significant size quantization (such as blue shifts in UV-vis spectra) was observed. Recently, TiO_2 clusters were synthesized using the DPA G4 template, and showed the quantum size effects [30]. A blue shift with decreasing particle size was observed, and the energy gap was dependent on the crystal form of the material. Using the proposed chemical bond method [31], the energy gap shift of spherical rutile and anatase cluster may be predicted, as shown in Figure 3 [15]. Consistency between the predictions and Satoh's experimental results [30] confirmed the accuracy of the chemical bond theory.

It can be seen from Figure 3(b)' inset that the energy gap shift ΔE approaches zero of the energy axis when $D>$ 6nm, which may explain why no blue shifts in UV-vis spectra were observed in Serpone's work [29]. Another interesting phenomena is that some anatase TiO_2 clusters show considerable redshift. For example, the energy shift ΔE is -0.31eV for anatase TiO_2 clusters with the size 0.95nm, causing the reduction of the energy gaps down to visible light range. It is known that the photoactivity of anatase TiO_2 is limited to the UV region, and how to extend the energy gap of TiO_2 into the visible range has attracted great interest. Doping seems an effective approach [42, 43], however, doped materials suffer from a thermal instability [32]. According to the calculated results, controlling the size of the semiconductor cluster may be a possible method to extend the energy gap of TiO_2 into visible region.

For rutile TiO_2 clusters with the size 1.0±0.2nm, 1.23±0.2nm and 1.49±0.2nm, the calculated average energy gap shift, 0.83eV, 0.55eV and 0.42eV, are very close to the corresponding experimental ones, 1.0eV, 0.6eV and 0.47eV, respectively. And for anatase TiO_2 clusters with size 1.09±0.2nm, 1.23±0.2nm and 1.57±0.2nm, the calculated average energy-gap shifts, 0.53eV, 0.52eV and 0.32eV, are also close to the corresponding experimental ones[41], 0.68eV, 0.47eV and 0.24eV, respectively. The calculated energy gap shift is the sum of the kubo energy shift and the surface energy shift, therefore, we can evaluate the variations of kubo and surface energy shift as a function of size for TiO_2 clusters separately.

As shown in Figure 3 [15], the kubo energy shift ΔE^{kubo} smoothly approaches to the bulk values with increasing size of the cluster. However, the curve of surface energy shift $\Delta E^{\text{surface}}$ shows an intense zigzag shape, which is almost the same with that of ΔE, suggesting that the shape of the energy gap shift curve is dominated by that of the surface energy gap shift.

ZnO is a versatile material that is bio-safe and biodegradable, and has been widely used in medical applications and environmental science.Like TiO_2 clusters, ZnO also shows quantum confinement effects in the experimentally accessible rage of sizes (<7 nm). The calculated energy gap shift of spherical ZnO nanocrystals with different diameters are listed in Table 2[44, 45]. It can be seen from the calculated results that the bond length of surface and inside atoms remain constant respectively during the variation of D for a given semiconductor, while the surface bond lengths of the nanocrystal are a little shorter than the inside ones because of surface reconstruction. Beside the effect of bond length, the effect of change in coordination number of surface atoms on band gap is also important based on the formulae. The valence electron densities of the surface bonds N_e are much higher that that of the inside ones due to the lower average coordination number N_c of the surface atoms. In addition, the heteropolar coulomb gap C of the surface bonds decrease by almost 3 times.

That's to say, the change of bond length, the coordination number of surface atoms as well as the heteropolar coulomb gap play important roles in band gap shift.

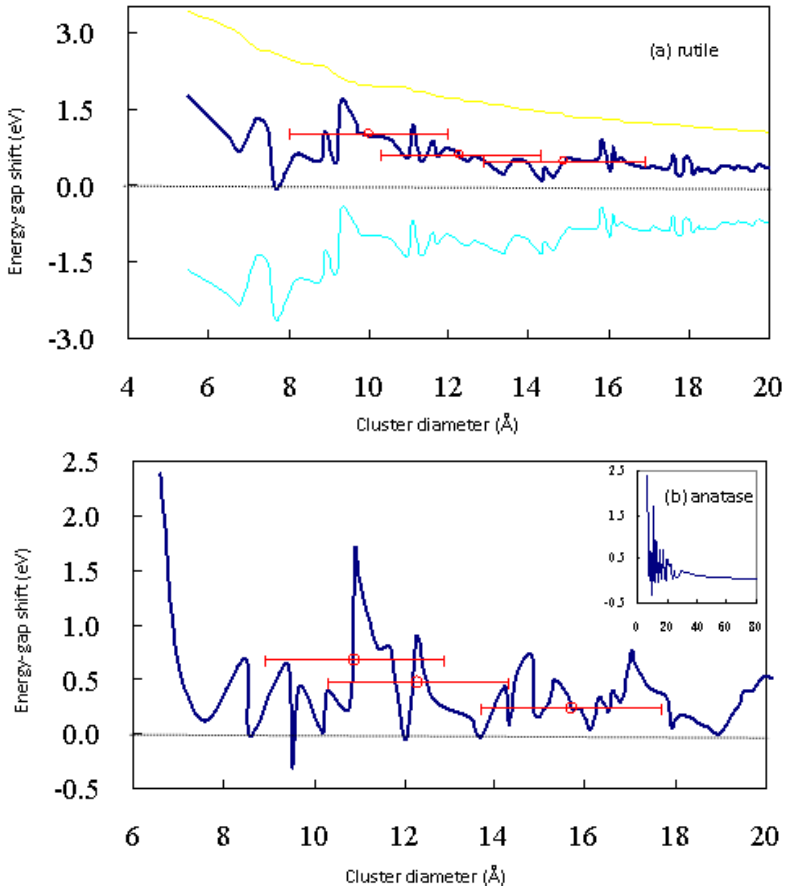

Figure 3. Dependence of energy-gap shifts of TiO_2 on cluster sizes and sturctures. Solid lines are the calculations of spherical clusters using the chemical bond theory. Open circles represent the experimental data[22]. (a) Rutile TiO_2 clusters:the blue, yellow and green lines represent energy-gap shift ΔE, kubo energy shift ΔE^{kubo} and surface energy shift $\Delta E^{surface}$, respectively. (b) Anatase TiO_2 clusters:the blue line represent energy-gap shift ΔE. Inset shows the trend of ΔE.

Although the surface atoms decrease with the reduced diameters, both the proportion of surface atoms to bulk atoms and the proportion of surface bonds $F^{surface}$ increase more obviously, which lead to a gradually enhanced surface effect and a higher energetic state of surface atoms. The transition energy from the valence to the conduction band increase, effectively increasing the band gap energy. According to the calculated results, $\Delta E^{surface}$ is more sensitive to $F^{surface}$ compared with$E_g^{surface}$ which remainsapproximatelyconstant during the variationof D. The relationship between $\Delta E^{surface}$ and $F^{surface}$ is almost linear for a given nanocrystal alloy.

Table 2. Theoretical data for the Spherical Nano ZnO clusters. N_c is average coordination number; energy-gap shift ΔE, kubo energy shift ΔE^{kubo} and surface energy shift $\Delta E^{surface}$ are in eV

D(Å)		d(Å)	N_e(Å^{-3})	N_c	C(eV)	E_h(eV)	E_g(eV)	ΔE^{kubo}	$\Delta E^{surface}$	ΔE
57. 5	inside	1.988	0.331	4.000	9.145	7.230	11.658	0.422	-0.316	0.106
	surface	1.930	0.544	2.659	3.678	7.781	8.607			
67. 5	inside	1.988	0.331	4.000	9.145	7.230	11.658	0.359	-0.268	0.092
	surface	1.930	0.547	2.641	3.622	7.781	8.583			
105	inside	1.988	0.331	4.000	9.145	7.230	11.658	0.231	-0.172	0.059
	surface	1.930	0.542	2.666	3.701	7.781	8.617			
120	inside	1.988	0.331	4.000	9.145	7.230	11.658	0.202	-0.151	0.051
	surface	1.930	0.543	2.663	3.693	7.781	8.613			

The Band Gap Shifts of Semiconductor Nanowires

Nanotechnology based on nanowires has opened up new directions in band gap engineering of optoelectronic devices. Among the III-V semiconductor nanowires, InP nanowires are one the most extensively investigated targets in recent years due to their potential applications in future nanoelectronic and nano-optoelectronic devices[46, 47]. Using the chemical bond theory, the energy-gap shifts of InP as well as Si nanowires are calculated and plotted against the number of stoms shown in Figure 4[31].

In order to study the quantum confinement effects of nanowires, three possible structural models of tapered and twinned InP nanowires were constructed and expressed as ABCABC, ABCACBA and ABCAACBA, as shown in Figure 4(a)-(c). The first structural model is a normal stacking sequence of zinc blende crystal where each letter represents a bilayer composed of a pair of one group III and one group V atom. The second model ABCACBA (here A is the twin plane) may lead to a straight-edged nanowire. And the third model ABCAACBA(AA are two sequential twin planes) may lead to a tapered-twinned nanowire. The wires grow in <111> direction. L and D are the length and diameter of nanowires, respectively.For nanowires, the large aspect ratio L/D may also play an important role in the shift of energy gaps besides the structural morphology [33]. For non-polar Si semiconductor nanowires, the straight-edge nanowires (red curve) have the biggest energy gap shift, while the tapered nanowires (blue curve) have the smallest ones. For polar InP nanowires, however, a totally reversed sequence of energy shift appears, i.e., the blue curve lies on top of one another. In addition, the difference between the curves of InP nanowires are significant greater than that of Si nanowires. The energy gap shifts in the straight and twinned InP nanowires tend to negative values, instead of decreasing toward zero like that of the tapered nanowires according to the calculated results, which is in agreement with Weert' experimental results[49, 50].

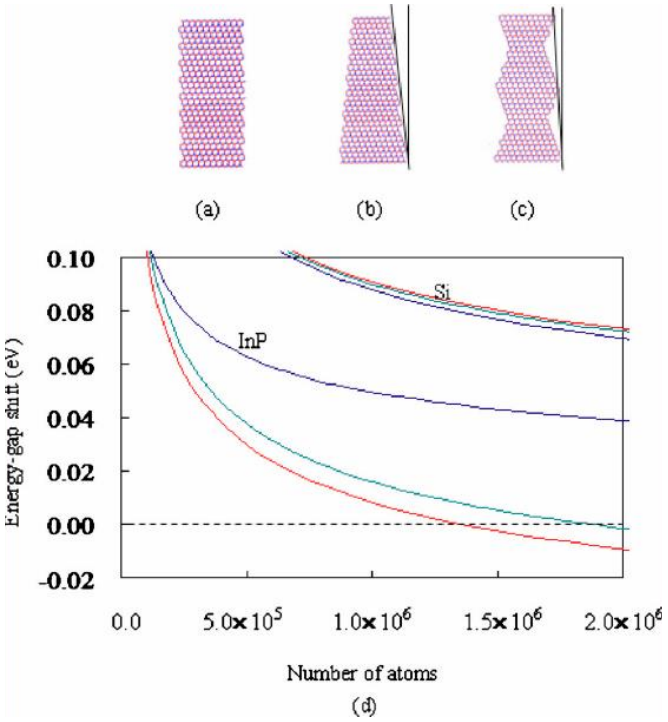

Figure 4. (a), (b) and (c) are the structure models of the straight-edge, tapered and the tapered-twinned InP nanowires along <111>, respectively. (d) The energy-gap shifts of the Si nanowires with diameter of 7nm and InP nanowires with diameter of 7.6nm. The red, green and blue curves represent the energy-gap shifts of the straight-edge, tapered and twinned nanowires, respectively [31].

Many other nanowires show similar large redshifts relative to energy gap of the bulk. According to Eq. (6), the energy gap shift is the result of a competition between the positive Kubo energy gap shift and thenegative surface energy gap shift. When aspect ratios $L/D \rightarrow \infty$, Kubo energy gap shift $\Delta E^{kubo} \rightarrow 0$, while the surface energy shift $\Delta E^{surface}$turn to negative values for both the straight and twinned InP nanowires with D = 7.6nm, which make the energies shift to red.

Further studies about the InP cubic nanowires of 5*5*L ,10*10*L , 20*20*L , 50*50*L and 100*100*L nm also show negative energy gap shift.

The Band Gap Shifts of Core/Shell Semiconductor Dots

For nanocrystals composed of a single material, the electronic properties can be tuned by the choice of material, size and shape. Additional control may be obtained using a core/shell structure where the type or thickness of the shell and core can tailor the optical, electronic, electrical and chemical properties of semiconductor nanocrystals. These core/shell quantum dots and nanowires allow a wide range of problems to be addressed, and have attracted much interest due to the notable potential applications in lasers and biomedicine. Some of the most interesting systems, for example ZnS, CdS shell and CdSe, CdTe core systems are widely studied in experiments. For core/shell quantum dots, the atoms of the core material have normal coordination. The kubo energy shift and surface energy shift can be written as[23]:

$$\Delta E^{kubo}(\text{core/shell}) = (m_e e^4/2\hbar^2)(V^{core} N_e^{core} + V^{shell} N_e^{shell})^{-1/3} \quad (19)$$

$$\Delta E^{surface}(\text{core/shell}) = F^{surface} [E_g{}^{surface}(\text{shell}) - E_g{}^{bulk}(\text{shell})] \quad (20)$$

The calculated energy gaps for the InP/ZnS, CdSe/CdS, CdSe/ZnS and CdTe/ZnS core/shell quantum dots are listed in Table 3, which are in agreement with the experimental values[51-54].

The Band Gap Shifts of Semiconductor Homogeneous Nanoalloys

Besides the size control, alloying could also tune the band gap by choosing the appropriate composition the materials and/or changing the ratio *x* of one component in nanocrystal alloys, since the interatomic interaction among different elements or compounds are different [55-61].

Table 3. Theoretical data for the core/shell nanocrystals. n_b is the number of bonds; calculated energy-gap $E_{g\,calc}$, experimental energy-gap $E_{g\,exp}$, kubo energy shift ΔE^{kubo} and surface energy shift $\Delta E^{surface}$ are in eV. *D*,*D*c and *D*s are diameter of nanocrystal, diameter of core and shell thickness in Å, respectively

Core/shell semiconductors	*D* (*D*c/*D*s) (Å)		n_b	ΔE^{kubo}	$\Delta E^{surface}$	$E_{g\,calc}$	$E_{g\,exp}$
InP/ZnS	45 (28/17)	inside	3518	0.649	-0.361	1.637	1.687
		surface	732				
CdSe/CdS	44 (37/7)	inside	2470	0.721	-0.438	2.014	2.049
		surface	583				
	51 (37/14)	inside	3903	0.629	-0.371	1.991	1.992
		surface	743				
	58 (37/21)	inside	6388	0.541	-0.313	1.960	1.966
		surface	1006				
	65 (37/28)	inside	9336	0.481	-0.279	1.934	1.946
		surface	1305				
	72 (37/35)	inside	13041	0.433	-0.248	1.918	1.927
		surface	1587				
CdSe/ZnS	50 (40/10)	inside	4196	0.583	-0.367	1.949	2.011
		surface	862				
	64 (40/24)	inside	10639	0.452	-0.257	1.927	1.989
		surface	1422				
CdTe/ZnS	45 (25/20)	inside	3526	0.649	-0.361	1.718	1.76
		surface	732				

Some alloy nanocrystals show higher luminescence efficiency and stability due to the larger particle size, higher crystallinity, highercovalency, lower inter-diffusion, and spatial composition fluctuation. These indicate that the band gap can be tuned and even be "designed" as hoped in applications by changing the nanocrystal diameters and the types or fractions of the components, while the stability of composite structures comprising different semiconductor materials can be greatly improved if compared with the plain nanocrystals. The chemical bond theory may be employed to study the band gap of semiconductor homogeneous alloyswith various size and compositions.

For semiconductor nanocrystal alloys, expressed as A_xB_{1-x} (*A* and *B* represent the two semiconductor crystals composing the alloy), the band gap $E_g(x, D)$ function is similar to that of single semiconductor and can be expressed as the sum of the band gap for bulk alloys and the band gap shift induced by the ratio *x* and the size *D*[34]:

$$E_g(x,D) = E_g\ (x,\infty) + \Delta E_g(x,D) \tag{21}$$

$E_g\ (x, \infty)$is a composition-dependent function for bulk nanocrystal alloys and usually can be expressed as the empirical formula[35] as follow based on the experimental data:

$$E_g(x,\infty) = E_g(0,\infty) + [E_g(1,\infty) - E_g(0,\infty) - b]x + bx^2 \tag{22}$$

where *b*, named the bowing parameter, is also a composition-dependent function when the alloy components have different lattice constants [36].

$$\Delta E_g(x,D) = \Delta E_g^{\text{kubo}}(x,D) + \Delta E_g^{\text{surface}}(x,D) \tag{23}$$

$$\Delta E^{\text{kubo}}(x,D) = (m_e e^4 / 2\hbar^2)[V(x,D)N_e(x,D)]^{-1/3} \tag{24}$$

$$\Delta E_g^{\text{surface}}(x,D) = \frac{n_A(x,D)}{n_A(x,D)+n_B(x,D)}\Delta E_{gA}^{\text{surface}}(D) + \frac{n_B(x,D)}{n_A(x,D)+n_B(x,D)}\Delta E_{gB}^{\text{surface}}(D) \tag{25}$$

here$n_A(x, D)$ and $n_B(x, D)$ are the bond numbers of semicondutor *A* and *B* in nanocrystal alloys, respectively. $\Delta E_{gA}^{\text{surface}}(D)$ and $\Delta E_{gB}^{\text{surface}}(D)$ are the surface effect shift part of nanocrystal *A* and *B* with diameter *D*, respectively, which can be calculated by formulae (6)-(18).

Since different nanocrystal structures and diameters of particle size will surely lead to different atom numbers of surface and inside nanocrystals, as well as the proportion F^{surface} of surface bonds, sphere models with different diameters and structures were built to determine the numbers of atoms and bonds. For the same crystal with different diameters, we suppose the bond lengths of surface and inside the crystal remain constant respectively. Here *D* values are selected base on the known experimental results of the nanocrystal alloys.

Table 4 listed the available experimental band gap functions of bulk alloys and the calculated band gap shifts and band gap energy in the range of x =0~1 with corresponding structure and diameter D. It can be seen thatE_g (x, D) increases with decreasing D for a given nanocrystal alloy, similar to the cases of single semiconductor compounds composing the alloy. Owing to that most of the E_g (x, ∞) for bulk nanosemiconductors alloy are definite, E_g (x, D) of nanosemiconductor alloys with different D are mainly determined by ΔE_g (x, D). For example, the ΔE_g (x, D) of zb-$(ZnS)_x(CdS)_{1-x}$varies from about 0.303 to 0.132eV when D increases from 4.4 to 9.0nm. The biggest and smallest ΔE_g (x, D) are 0.499eV for zb-$(CdS)_x(CdSe)_{1-x}$ nanocrystal alloy with D = 2.8nm and 0.121eV for zb-$(ZnSe)_x(CdSe)_{1-x}$ with D = 10.0nm, respectively. The energy gap shift show obvious size-dependent properties, especially for the nanosemiconductor alloys with the size of several nanometers.

Table 4. The experimental band gap functions of bulk alloys and the calculated band gap shift and band gap with corresponding *D*[34]

Alloy	$E_g(x,\infty)$ (eV)	*D*(nm)	*x*	$\Delta E_g(x,D)$ (eV)	$E_g(x,D)$ (eV)
zb-$(ZnS)_x(CdS)_{1-x}$	$2.460+0.439x+0.827x^2$ [37]	4.4	0~1	0.259~0.303	2.719~4.029
		9.0		0.132~0.150	2.592~3.876
w-$(ZnS)_x(CdS)_{1-x}$	$2.501+0.328x+0.921x^2$ [37]	4.8		0.250~0.280	2.751~4.030
		5.8		0.200~0.230	2.701~3.980
		6.4		0.179~0.211	2.680~3.961
		8.0		0.131~0.169	2.632~3.919
zb-$(CdS)_x(CdSe)_{1-x}$	$1.74+0.49x+0.3x^2$ [38]	2.8		0.499~0.395	2.239~2.925
		3.1		0.480~0.378	2.220~2.908
		3.6		0.417~0.295	2.157~2.825
		4.3		0.343~0.260	2.083~2.790
		5.8		0.256~0.203	1.996~2.733
zb-$(ZnSe)_x(CdSe)_{1-x}$	$1.675+0.659+0.387x^2$ [37]	10.0		0.150~0.124	1.825~2.845
				0.136~0.121	1.811~2.842
w-$(ZnSe)_x(CdSe)_{1-x}$	$1.74+0.51x+0.35x^2$ [39]	5.2		0.265~0.246	2.005~2.846
		5.8		0.241~0.222	1.981~2.822
		6.3		0.228~0.202	1.968~2.802
		6.8		0.209~0.190	1.949~2.790
		7.5		0.192~0.172	1.932~2.772
w-$(CdSe)_x(CdTe)_{1-x}$	$1.43-0.553x+0.862x^2$ [40]	3.5		0.433~0.406	1.863~2.145
		5.0		0.316~0.292	1.746~2.031
		6.5		0.241~0.224	1.671~1.963

Beside the size effects, the compositions of the alloys also perform an important function in the shift of the energy gap. Taking zb-$(CdS)_x(CdSe)_{1-x}$ with D=2.8nm for example, the energy gap shift changes from 0.499 to 0.395 eV when x varies from 0 to 1. When D increases to 5.8nm, the energy gap shift varies from 0.256 to 0.203 in the range of x=0~1. With the increased D, the energy shift changes less along with x. Generally, the effect of

composition on energy gap shift is not as significant as the size effect, however, the composition-dependent energy shift is considerable large for both the bulk and nanoscaled semiconductors. With the change of *x*, for instance, the energy gap shift expand 1.266, 1.310, and 1.284 eV for bulk zb-$(ZnS)_x(CdS)_{1-x}$ and nanoscaled alloys with D = 4.4 and 9nm, respectively. Therefore, in some cases, if adjusting size may result in system instability or hard fabrication, modulating composition can avoid these drawbacks and meantime satisfy the same desirable band gap energy of nanocompounds.

Figures 5-9 show comparisons of the theoretical $E_g(x, D)$ functions (solid lines) for nanosemiconductor alloys and available experimental results (symbols)[34]. The *x*-axis represents composition change from pure nanocrystal with smaller energy gap to another pure nanocrystal with bigger one.

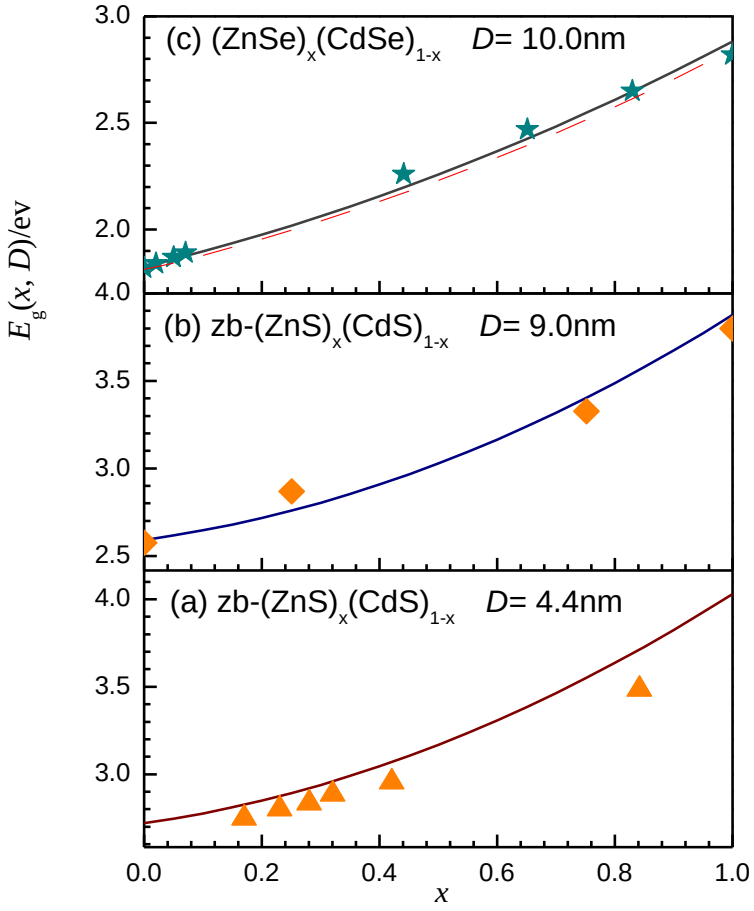

Figure 5. $E_g(x, D)$ functions for zb-$(ZnS)_x(CdS)_{1-x}$ nanocrystal alloys with the diameters of (a) 4.4 and (b) 9.0nm, and $(ZnSe)_x(CdSe)_{1-x}$ with the diameter of (c)10.0nm, respectively. The solid lines represent the calculated band gap energies of zinc blende structure.The red dashed line in (c) denotes the calculated band gap energy of $(ZnSe)_x(CdSe)_{1-x}$ with wurtzite structure. The experimental results are denoted by ▲[43], ◆[64] and★[44], respectively[34].

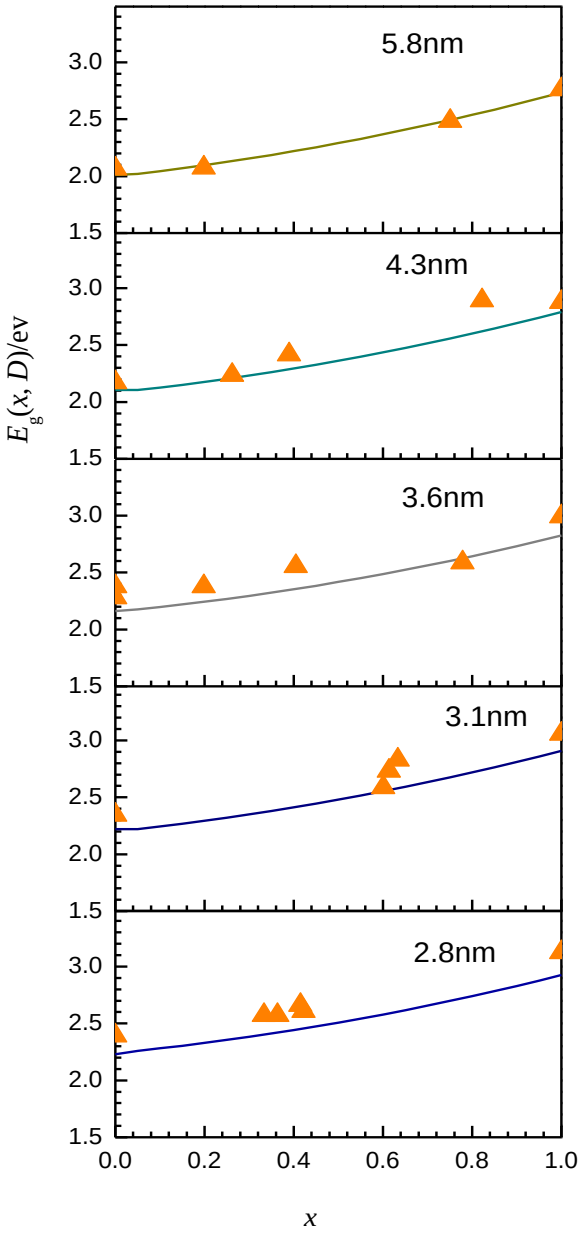

Figure 6. $E_g(x,D)$ functions for zb-$(CdS)_x(CdSe)_{1-x}$ nanocrystal alloy with the diameters of 2.8, 3.1, 4.3, 3.6 and 5.8nm, respectively. The solid lines denote the calculated band gaps, and the symbols represent the experimental results [38].

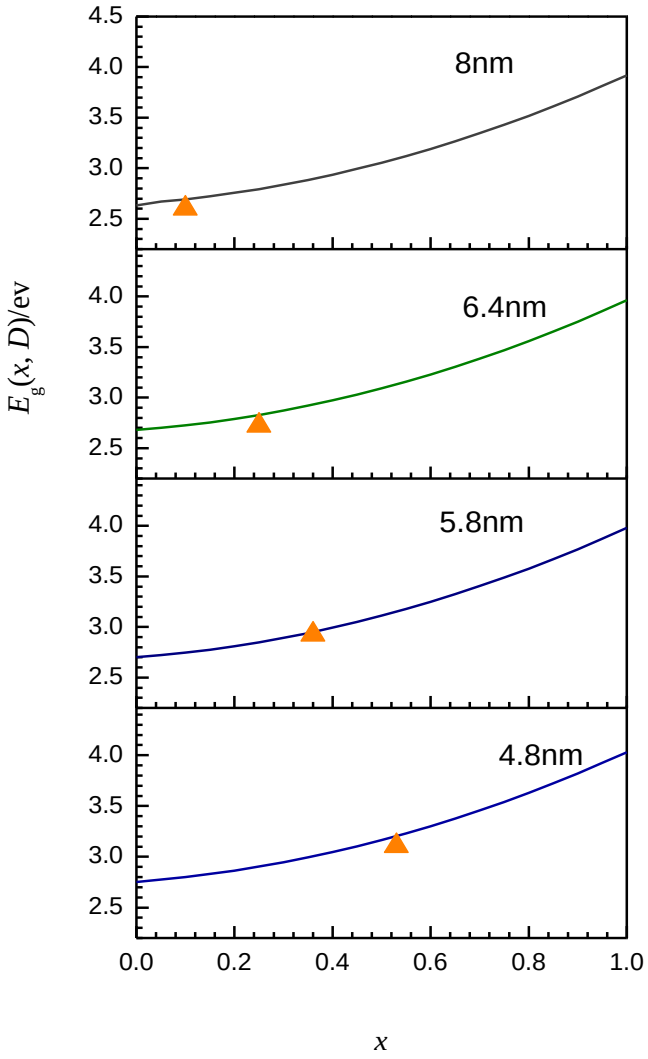

Figure 7. $E_g(x,D)$ functions for w-$(ZnS)_x(CdS)_{1-x}$ nanocrystal alloy with the diameters of 4.8, 5.8, 6.4 and 8.0nm, respectively. The solid lines denote the calculated band gaps and the symbols represent the experimental results [47].

(ZnSe)x(CdSe)1-x alloys show higher luminescence and stability compared to the case for the components with narrower energy gaps. For (ZnSe)x(CdSe)1-x bulk alloy, it is believed that there is a structural phase transition from wurtzite to zinc-blende structure approximately in the composition region $0.3<x<0.7$[45]. While it is also reported that MBE-grown (ZnSe)x(CdSe)1-x layers on GaAs(100) result in films of the zinc-blende structure over the whole composition range[46]. However, the differences between the calculated results for nanosemiconductors with zinc-blende and wurtize structures are comparable small that can be neglected. For example, the discrepancies of energy shift are 0.003eV for zb-ZnSe and w-ZnSe and 0.022eV for zb-CdSe and w-CdSe semiconductor particles with D=10nm, respectively. In addition, the experimental values of the bowing

factors and energy gap shift are almost the same for nanosemiconductors with these two different structures. The comparison between the available experimental and calculated energy gaps of (ZnSe)x(CdSe)1-x with zinc blende structure (solid line) and wurtzite structure (red dashed line) are plotted in Fig. 2, where it can seen that the discrepancy of energy gap is much small, indicating that it is it is acceptable to neglect the phase transition and take zine blende or wurtzite structure as model for calculation yet without great error.

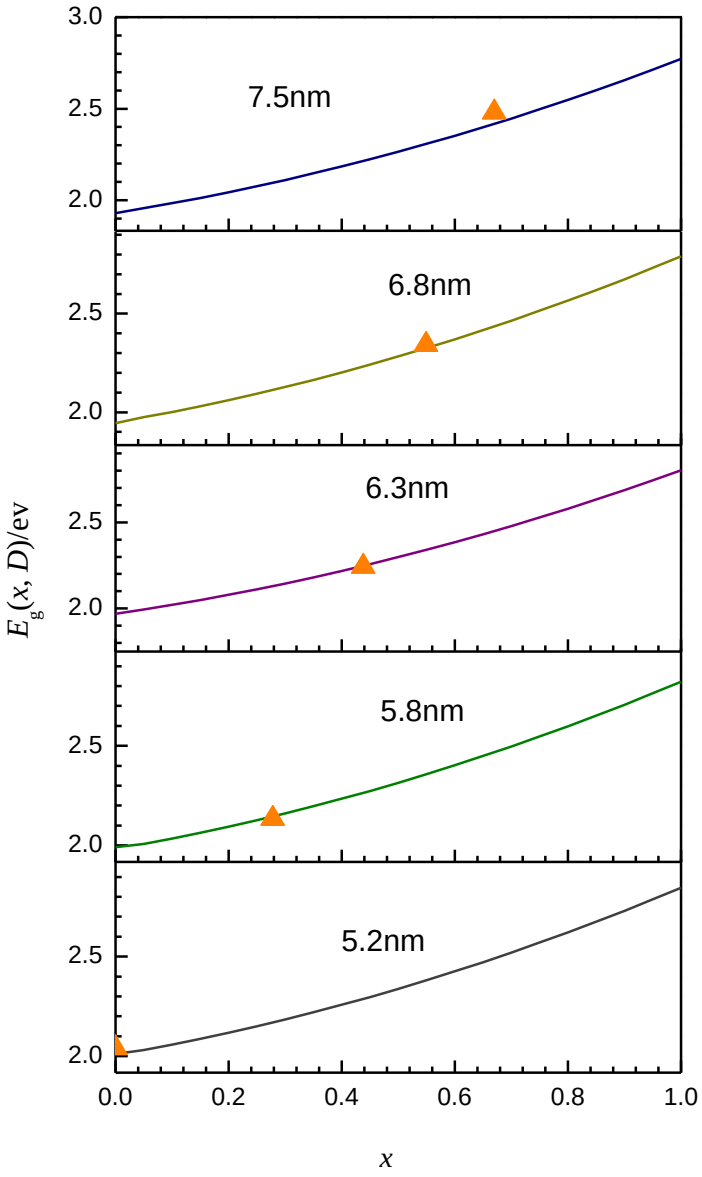

Figure 8. $E_g(x, D)$ functions for w-$(ZnSe)_x(CdSe)_{1-x}$ nanocrystal alloy with the diameters of 5.2, 5.8, 6.3, 6.8 and 7.5nm, respectively. The symbols represent the experimental results [48].

Figures 6-9 show the energy gap functions for homogeneous zb-$(CdS)_x(CdSe)_{1-x}$, w-$(ZnS)_x(CdS)_{1-x}$, w-$(ZnSe)_x(CdSe)_{1-x}$ and w-$(CdSe)_x(CdTe)_{1-x}$ alloys with different diameters. There are considerable good agreements between the available experimental and calculated results. The surface effect will become weaker with increasing *D*, which may induce large discrepancy in calculation due to the close relationship between the surface properties and the band gaps. The nanocrystal alloys with high quality and small diameters are difficult to synthesize, while the chemical bond model can provide prediction and theoretical guidance before the synthesis.

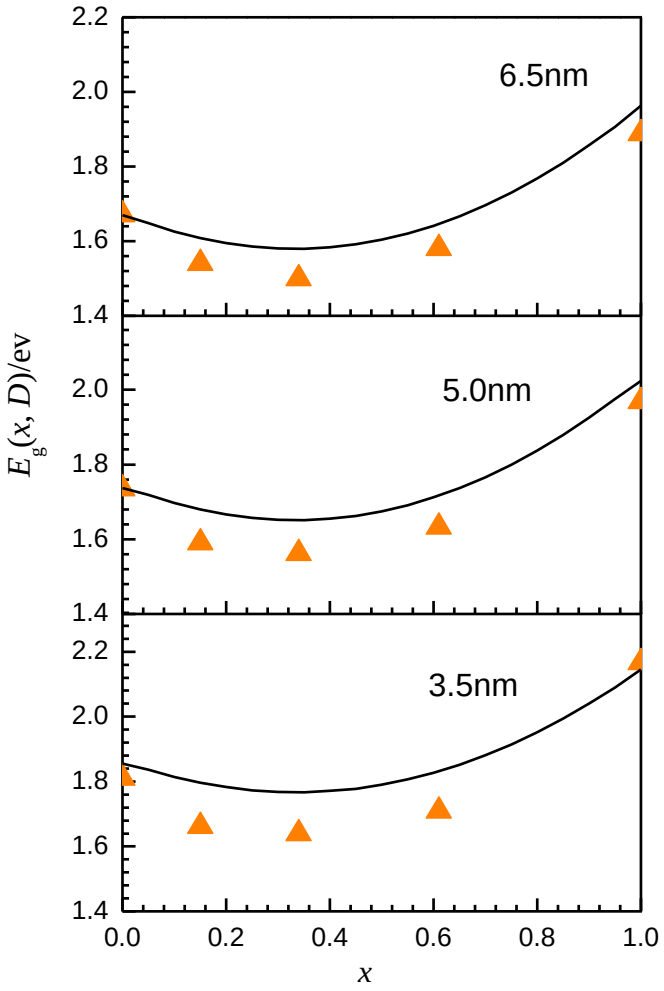

Figure 9. $E_g(x, D)$ functions for w-$(CdSe)_x(CdTe)_{1-x}$ with *D* =3.5, 5.0, and 6.5nm, respectively. The symbols represent the experimental results [49].

Conclusion

In summary, a few theories for quantum size effect are reviewed. In particular, a chemical bond method of quantum size effect is introduced in detail.It can be used to calculate the energy gap shift and further the energy gap of single nanocrystals particles, nanowires, core/shell semiconductors, semiconductor homogeneousalloys. The calculation may be carried out on a pocket calculator. Its simplicity stems from incorporating the quantum mechanical effects and surface effects into chemical bond properties via algebraic relationships rather than through variationalsolutions of the wave equation. It will provide guide to design the materials with expected properties.

This work is supported by the National Natural Science Foundation of China (Grant 21371149).

References

[1] A. L. Efros, *Soviet Physics Semiconductors Ussr* 16 (7), 772-775 (1982).
[2] Y. Wang and N. Herron, *The Journal of Physical Chemistry* 95 (2), 525-532 (1991).
[3] M. V. Rama Krishna and R. A. Friesner, *Physical Review Letters* 67 (5), 629-632 (1991).
[4] M. V. Rama Krishna and R. A. Friesner, *The Journal of Chemical Physics* 96 (2), 873-877 (1992).
[5] S. I. Pokutnyĭ, *Semiconductors* 41 (11), 1323-1328 (2007).
[6] S. I. Pokutnyi, *Semiconductors* 47 (6), 791-798 (2013).
[7] S. I. Pokutnyi, *Semiconductors* 46 (2), 165-170 (2012).
[8] S. Öğüt, J. R. Chelikowsky and S. G. Louie, *Physical Review Letters* 79 (9), 1770-1773 (1997).
[9] Y. Wang, A. Suna, W. Mahler and R. Kasowski, *The Journal of Chemical Physics* 87 (12), 7315-7322 (1987).
[10] P. E. Lippens and M. Lannoo, *Physical Review* B 39 (15), 10935-10942 (1989).
[11] S. Y. Ren and J. D. Dow, *Physical Review* B 45 (12), 6492-6496 (1992).
[12] L. W. Wang and A. Zunger, *Physical Review* B 51 (24), 17398-17416 (1995).
[13] G. Y. Wu, T. C. McGill, C. Mailhiot and D. L. Smith, *Physical Review* B 39 (9), 6060-6070 (1989).
[14] D. Bera, L. Qian, T.-K. Tseng and P. H. Holloway, *Materials* 3 (4), 2260-2345 (2010).
[15] F. Gao, *Inorganic Chemistry* 49 (22), 10409-10414 (2010).
[16] M. G. Mason, *Physical Review* B 27 (2), 748-762 (1983).
[17] C. Q. Sun, *Physical Review* B 69 (4), 045105 (2004).
[18] J. C. Phillips, *Reviews of Modern Physics* 42 (3), 317-356 (1970).
[19] J. A. Van Vechten, *Physical Review* 187 (3), 1007-1020 (1969).
[20] F. Gao, J. He, E. Wu, S. Liu, D. Yu, D. Li, S. Zhang and Y. Tian, *Physical ReviewLetters* 91 (1), 015502 (2003).
[21] T. K. Bergstresser and M. L. Cohen, *Physical Review* 164 (3), 1069-1080 (1967).
[22] T. Trindade, P. O'Brien and X.-m. Zhang, *Chemistry of Materials* 9 (2), 523-530 (1997).

[23] C. B. Murray, D. J. Norris and M. G. Bawendi, *Journal of the American ChemicalSociety* 115 (19), 8706-8715 (1993).
[24] J. Nanda, S. Sapra, D. D. Sarma, N. Chandrasekharan and G. Hodes, *Chemistry ofMaterials* 12 (4), 1018-1024 (2000).
[25] H. Fu and A. Zunger, Physical Review B 56 (3), 1496-1508 (1997).
[26] A. A. Guzelian, U. Banin, A. V. Kadavanich, X. Peng and A. P. Alivisatos, *Applied Physics Letters* 69 (10), 1432-1434 (1996).
[27] M. A. Malik, M. Afzaal, P. O'Brien, U. Bangert and B. Hamilton, *Materials Scienceand Technology* 20 (8), 959-963 (2004).
[28] M. A. Olshavsky, A. N. Goldstein and A. P. Alivisatos, *Journal of the AmericanChemical Society* 112 (25), 9438-9439 (1990).
[29] N. Serpone, D. Lawless and R. Khairutdinov, *The Journal of Physical Chemistry* 99 (45), 16646-16654 (1995).
[30] N. Satoh, T. Nakashima, K. Kamikura and K. Yamamoto, *Nat Nano* 3 (2), 106-111 (2008).
[31] F. Gao, *Applied Physics Letters* 98 (19), - (2011).
[32] R. Asahi, T. Morikawa, T. Ohwaki, K. Aoki and Y. Taga, *Science* 293 (5528), 269-271 (2001).
[33] C. N. R. Rao, G. U. Kulkarni, A. Govindaraj, B. C. Satishkumar and P. J. Thomas, *Pure and Applied Chemistry* 72 (1-2), 21-33 (2000).
[34] L. Gao and F. Gao, *Applied Physics Letters* 103 (5), 0531011-0531014 (2013).
[35] A. G. Thompson and J. C. Woolley, *Canadian Journal of Physics* 45 (2), 255-261 (1967).
[36] R. Hill and D. Richardson, Journal of Physics C: *Solid State Physics* 6 (5), L115 (1973).
[37] S. Adachi, *Properties of Semiconductor Alloys: Group-IV, III-V, II-VI, semiconductors*. (John Wiley & Sons, Ltd, West Sussex, 2009).
[38] L. A. Swafford, L. A. Weigand, M. J. Bowers, J. R. McBride, J. L. Rapaport, T. L. Watt, S. K. Dixit, L. C. Feldman and S. J. Rosenthal, *Journal of the American Chemical Society* 128 (37), 12299-12306 (2006).
[39] J. U. Kim, J. J. Lee, H. S. Jang, D. Y. Jeon and H. Yang, *Journal of Nanoscience andNanotechnology* 11 (1), 725-729 (2011).
[40] J. B. Mullin, edited by R. K. Willardson and H. L. *Goering* (Reinhold, New York, 1962), Vol. 1.
[41] S. Guha, B. J. Wu, H. Cheng and J. M. DePuydt, *Applied Physics Letters* 63 (15), 2129-2131 (1993).
[42] Y. F. Zhu, X. Y. Lang and Q. Jiang, *Advanced Functional Materials* 18 (9), 1422-1429 (2008).
[43] X. Zhong, S. Liu, Z. Zhang, L. Li, Z. Wei and W. Knoll, *Journal of MaterialsChemistry* 14 (18), 2790-2794 (2004).
[44] J.-P. Ge, S. Xu, J. Zhuang, X. Wang, Q. Peng and Y.-D. Li, *Inorganic Chemistry* 45 (13), 4922-4927 (2006).
[45] A. S. Nasibov, Y. V. Korostelin, P. V. Shapkin, L. G. Suslina, D. L. Fedorov and L. S. Markov, *Solid State Communications* 71 (10), 867-869 (1989).
[46] N. Samarth, H. Luo, J. K. Furdyna, R. G. Alonso, Y. R. Lee, A. K. Ramdas, S. B. Qadri and N. Otsuka, *Applied Physics Letters* 56 (12), 1163-1165 (1990).

[47] X. Zhong, Y. Feng, W. Knoll and M. Han, *Journal of the American Chemical Society* 125 (44), 13559-13563 (2003).

[48] X. Zhong, M. Han, Z. Dong, T. J. White and W. Knoll, *Journal of the AmericanChemical Society* 125 (28), 8589-8594 (2003).

[49] R. E. Bailey and S. Nie, *Journal of the American Chemical Society* 125 (23), 7100-7106 (2003).